7th Workshop on Numerical Methods in Applied
Science and Engineering (NMASE 08)
Vall de Núria, 9 a 11 de enero de 2008

STRICT ERROR BOUNDS IN LINEAR SOLID MECHANICS USING A SUBDOMAIN-BASED FLUX-FREE APPROACH

Régis Cottereau[1,2,*] and Pedro Díez[2]

1: International Center for Numerical Methods in Engineering (CIMNE)
E. T. S. d'Enginyers de Camins, Canals i Ports de Barcelona
Universitat Politècnica de Catalunya
web: http://www.cimne.upc.es

2: Laboratori de Càlcul Numèric
Departament de Matemàtica Aplicada III
Universitat Politècnica de Catalunya
e-mail: regis.cottereau,pedro.diez@upc.edu, web:http://www-lacan.upc.es

Key words: Error estimation, Error bounds, Residual-based estimators, Functional outputs.

Abstract. *In this paper, we derive, in the framework of the flux-free method, strict bounds for the energy norm of the error associated to a finite element computation. In that framework, and when using linear elements, the problems posed on the subdomains are solvable only when modified by the introduction of a projection operator in the residual. We introduce a new such operator, and show that, in the context of a dual formulation, it further allows to construct statically admissible fields over each subdomain. When combined, these local stress fields provide the desired strict bound.*

1 Introduction

In the past few decades, research and industry in the field of mechanics have relied increasingly on computational tools. The models and the resolution methods have grown increasingly complex and their careful assessment has become unavoidable. This task can be separated in two steps, which are grouped under the general denomination of Verification & Validation [1]. The validation step refers to the process of comparing the output of a mathematical/mechanical model to experimental results and assessing its adequacy. The verification step, which usually precedes the validation, deals with the accuracy of the numerical treatment of the mathematical/mechanical model. It is commonly referred to as the error estimation step and sets the general framework for this paper.

Historically, error estimation initially relied on *a priori*, or explicit, methods, whose goal is to assess the accuracy of a computational output before actually running the

computation, using only data such as the geometry, discretization and mechanical parameters. However, the bounds hence provided usually depend on constants that cannot be evaluated explicitely, therefore giving trends rather than estimations. Later works focused rather on *a posteriori*, or implicit, error estimation methods, where the output of the computation is also used to assess its accuracy. Three main groups of methods (see [2] for a more detailed review) arose: one based on the so-called constitutive relation error, by Ladevève and co-workers (see for example [3]); another based on the comparison of the discontinuous stress field computed by the FE method and a regularized version, following the leading work of Zienkiewicz and Zhu [4]; and, finally, a large family of methods, generically called equilibrated residual, or subdomain-based, methods, where the global residual problem of estimating the error in the original computation is replaced by a series of smaller local problems with appropriate boundary conditions (see for example [5, 6, 7, 8], and comparisons between approaches in [9, 10]). In this paper, we will concentrate on the so-called flux-free techniques [5, 11, 12, 13, 14, 10], that fall within this third group of methods, and we will follow more particularly the approach described in [15, 10].

In most of these subdomain-based methods, although the local problems are posed on smaller geometrical spaces, the functional spaces involved are still infinite-dimensional. The exact error is therefore replaced by the solution of a refined problem, and the bounds are given with respect to this solution. Hence the bounds are meaningful only as long as the solution of the refined problem is close enough to the exact error, and the methods are referred to as asymptotic. However, it is much more interesting, from an engineering point of view, to be able to provide strict bounds, that is to say with respect to the exact error. A dual formulation based on the principle of minimizing the complementary energy was proposed to attain that goal in the context of hybrid-flux residual estimators [16, 17]. Its extension to the flux-free methodology with linear elements, which is very common in practice, is not straightforward because issues of solvability of the local problems arise.

The objective of this paper is therefore to present the derivation of strict bounds for the error in an elasticity problem using a subdomain-based flux-free method. A particular emphasis will be put on the introduction of a new projection operator, which ensures, when using linear finite elements, the solvability of the local problems, as well as the construction of the statically admissible stress fields required to derive the strict bounds for the error. After the description of the model problem in Section 2, the flux-free methodology for the derivation of asymptotic bounds is recalled in Section 3. This section also introduces the new projection operator, which is compared to one that was previously derived [10]. Section 4 then concentrates on the derivation of strict bounds of the error, in the context of the flux-free method, and using the previously derived projection operator. Finally, some preliminary results in 2D-elasticity are presented in Section 5.

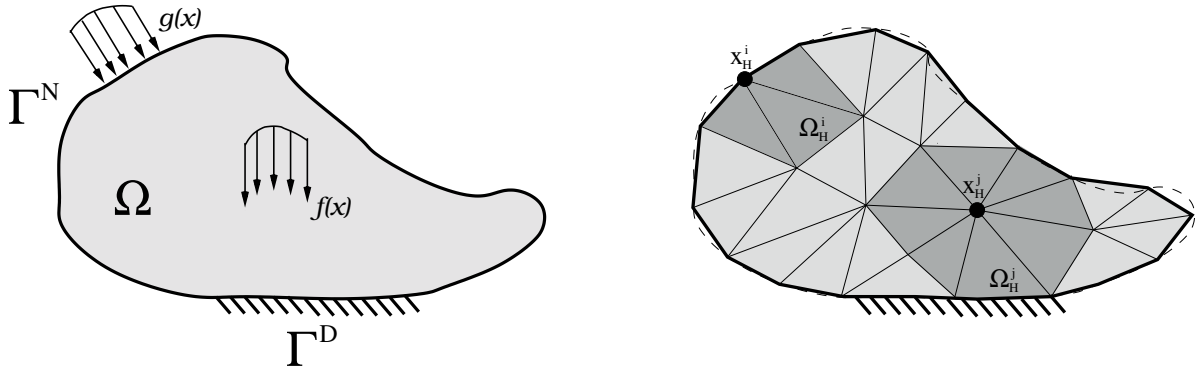

Figure 1: Model of the problem on the domain Ω, with internal loads $\boldsymbol{f}$, boundary forces $\boldsymbol{g}$ on Γ^{N} and blocked on Γ^{D} (left); and corresponding finite element triangulation $\mathcal{T}_H$ with two stars in darker tones, Ω_H^i and Ω_H^j, corresponding to nodes $\boldsymbol{x}_H^i$ and $\boldsymbol{x}_H^j$, respectively (right).

2 Model problem and main notations

As indicated in the introduction, we do not consider a "real-life" system, and start directly from a mathematical/mechanical model of a continuous medium. In this section, the main notations are introduced, as well as the strong and weak formulations of the problem.

2.1 Strong formulation of the problem

We consider an elastic polygonal domain $\Omega \subset \mathbb{R}^{n_d}$. The boundary, $\Gamma = \partial\Omega$, is divided into two complementary disjoint parts Γ^{D} and Γ^{N}, where essential and Neumann boundary conditions are imposed, respectively. Furthermore, the boundary Γ^{D} is assumed to be a non-empty set. The boundary value problem to be solved reads: find $\overline{\boldsymbol{u}} : \Omega \to \mathbb{R}^{n_d}$, such that

$$\begin{cases} \mathrm{Div}_{\boldsymbol{x}}\boldsymbol{\sigma}(\overline{\boldsymbol{u}}) + \overline{\boldsymbol{f}} = \boldsymbol{0} & \text{in } \Omega \\ \boldsymbol{\sigma}(\overline{\boldsymbol{u}}) \cdot \boldsymbol{n} = \overline{\boldsymbol{g}} & \text{on } \Gamma^{\mathrm{N}} \\ \overline{\boldsymbol{u}} = \boldsymbol{u}_{\mathrm{D}} & \text{on } \Gamma^{\mathrm{D}} \end{cases}, \tag{1}$$

where the internal force per unit volume $\overline{\boldsymbol{f}} \in [\mathcal{H}^{-1}(\Omega)]^{n_d}$, the Neumann boundary tractions $\overline{\boldsymbol{g}} \in [\mathcal{H}^{-1/2}(\Gamma^{\mathrm{N}})]^{n_d}$, and the imposed Dirichlet boundary displacement, $\boldsymbol{u}_{\mathrm{D}} \in [\mathcal{H}^{1/2}(\Gamma^{\mathrm{D}})]^{n_d}$ are given, $\mathcal{H}^{\alpha}(\mathcal{A})$ are the standard α-Sobolev spaces over $\mathcal{A}$, and $\boldsymbol{n}$ is the outgoing normal vector of Ω.

Introducing $\boldsymbol{u} \in [\mathcal{H}^1(\Omega)]^{n_d}$, such that $\boldsymbol{u}_{|\Gamma^{\mathrm{D}}} = \boldsymbol{u}_{\mathrm{D}}$, where $\boldsymbol{u}_{|\Gamma^{\mathrm{D}}}$ is the trace of $\boldsymbol{u}$ on Γ^{D}, $\boldsymbol{f} = \overline{\boldsymbol{f}} + \mathrm{Div}_{\boldsymbol{x}}\boldsymbol{\sigma}(\boldsymbol{u}_{\mathrm{D}})$, and $\boldsymbol{g} = \overline{\boldsymbol{g}} - \boldsymbol{\sigma}(\boldsymbol{u}_{\mathrm{D}}) \cdot \boldsymbol{n}$, the problem (1) can be replaced by: find $\boldsymbol{u} : \Omega \to \mathbb{R}^{n_d}$, such that

$$\begin{cases} \mathrm{Div}_{\boldsymbol{x}}\boldsymbol{\sigma}(\boldsymbol{u}) + \boldsymbol{f} = \boldsymbol{0} & \text{in } \Omega \\ \boldsymbol{\sigma}(\boldsymbol{u}) \cdot \boldsymbol{n} = \boldsymbol{g} & \text{on } \Gamma^{\mathrm{N}} \\ \boldsymbol{u} = \boldsymbol{0} & \text{on } \Gamma^{\mathrm{D}} \end{cases}, \tag{2}$$

thereby avoiding the notational complexity introduced by the inhomogeneous Dirichlet boundary conditions.

2.2 Weak formulation of the problem

We define $\boldsymbol{\mathcal{V}} = \{\boldsymbol{v} \in [\mathcal{H}^1(\Omega)]^{n_d}, \boldsymbol{v}_{|\Gamma^{\mathrm{D}}} = \boldsymbol{0}\}$, the space of admissible fields, the second order strain tensor $\boldsymbol{\epsilon}(\boldsymbol{v})$, which is defined as the symmetric part of the gradient tensor $\boldsymbol{\nabla v}$, so that $\boldsymbol{\epsilon}(\boldsymbol{v}) = \frac{1}{2}(\boldsymbol{\nabla v} + (\boldsymbol{\nabla v})^T)$, and the stress tensor $\boldsymbol{\sigma}(\boldsymbol{w})$, which is related to the strain tensor through a linear constitutive relation of the form, $\boldsymbol{\sigma}(\boldsymbol{w}) = \mathbb{C} : \boldsymbol{\epsilon}(\boldsymbol{w})$, where $\mathbb{C}$ is the fourth order, symmetric, positive-definite, elasticity tensor ($\mathbb{C}_{ijkl} = \mathbb{C}_{klij} = \mathbb{C}_{jikl}$, $1 \leq i, j, k, l \leq n_d$, and $\mathbb{C}_{ijkl}\boldsymbol{e}_{ij}\boldsymbol{e}_{kl} \geq \alpha \boldsymbol{e}_{ij}\boldsymbol{e}_{ij}$, $\alpha > 0$, for any second-order real symmetric tensor $\boldsymbol{e}$).

The weak formulation of the problem (2) states: find $\boldsymbol{u} \in \boldsymbol{\mathcal{V}}$, such that

$$a_\Omega(\boldsymbol{u}, \boldsymbol{v}) = l(\boldsymbol{v}), \quad \forall \boldsymbol{v} \in \boldsymbol{\mathcal{V}}, \tag{3}$$

where $a_\Omega : [\mathcal{H}^1(\Omega)]^{n_d} \times [\mathcal{H}^1(\Omega)]^{n_d} \to \mathbb{R}$ is the symmetric positive definite bilinear form given by

$$a_\Omega(\boldsymbol{w}, \boldsymbol{v}) = \int_\Omega \boldsymbol{\sigma}(\boldsymbol{w}) : \boldsymbol{\epsilon}(\boldsymbol{v}) \, d\Omega,$$

and $\ell : [\mathcal{H}^1(\Omega)]^{n_d} \to \mathbb{R}$ is the linear forcing functional, defined by

$$\ell(\boldsymbol{v}) = \int_\Omega \boldsymbol{f} \cdot \boldsymbol{v} \, d\Omega + \int_{\Gamma^{\mathrm{N}}} \boldsymbol{g} \cdot \boldsymbol{v}_{|\Gamma^{\mathrm{N}}} \, d\Gamma.$$

For $\boldsymbol{u} \in [\mathcal{H}^{-1}(\Omega)]^{n_d}$ and $\boldsymbol{v} \in [\mathcal{H}^1(\Omega)]^{n_d}$, we introduce the notation $\langle \boldsymbol{u}, \boldsymbol{v} \rangle_\Omega = \int_\Omega \boldsymbol{u} \cdot \boldsymbol{v} \, d\Omega$, and for $\boldsymbol{u} \in [\mathcal{H}^{-1/2}(\Gamma^{\mathrm{N}})]^{n_d}$ and $\boldsymbol{v} \in [\mathcal{H}^{1/2}(\Gamma^{\mathrm{N}})]^{n_d}$, we introduce the notation $\langle \boldsymbol{u}, \boldsymbol{v} \rangle_{\Gamma^{\mathrm{N}}} = \int_{\Gamma^{\mathrm{N}}} \boldsymbol{u} \cdot \boldsymbol{v} \, d\Gamma$. We observe that $\ell(\boldsymbol{v}) = \langle \boldsymbol{f}, \boldsymbol{v} \rangle_\Omega + \langle \boldsymbol{g}, \boldsymbol{v}_{|\Gamma^{\mathrm{N}}} \rangle_{\Gamma^{\mathrm{N}}}$. Note that, in general, we will drop the indication of the trace, and write simply $\langle \boldsymbol{g}, \boldsymbol{v} \rangle_{\Gamma^{\mathrm{N}}}$ for the latter product. For a given operator $\Pi : [\mathcal{H}^1(\Omega)]^{n_d} \to [\mathcal{H}^1(\Omega)]^{n_d}$, we then define the adjoint operators $\Pi^{\Omega *}, \Pi^{\Gamma^{\mathrm{N}} *} : [\mathcal{H}^{-1}\Omega)]^{n_d} \to [\mathcal{H}^{-1}(\Omega)]^{n_d}$ such that $\langle \boldsymbol{u}, \Pi \boldsymbol{v} \rangle_\Omega = \langle \Pi^{\Omega *} \boldsymbol{u}, \boldsymbol{v} \rangle_\Omega$, and $\langle \boldsymbol{u}_{|\Gamma^{\mathrm{N}}}, \Pi \boldsymbol{v}_{|\Gamma^{\mathrm{N}}} \rangle_{\Gamma^{\mathrm{N}}} = \langle \Pi^{\Gamma^{\mathrm{N}} *} \boldsymbol{u}, \boldsymbol{v} \rangle_\Omega$. Finally, throughout the paper, the energy norm induced by the bilinear form $a_\Omega(\cdot, \cdot)$ will be denoted $\| \cdot \|_\Omega$, that is, $\|\boldsymbol{v}\|_\Omega^2 = a_\Omega(\boldsymbol{v}, \boldsymbol{v})$.

The Lax-Milgram theorem ensures that Eq. (3) has a unique solution in $\boldsymbol{\mathcal{V}}$, that we will denote $\boldsymbol{u}_{\mathrm{ex}}$. However this solution is usually not available analytically, and we will use the FE method to compute an approximation.

2.3 Finite Element solution of the problem

We therefore introduce a triangulation, $\mathcal{T}_H$, of Ω, whose elements and vertices are denoted, respectively, $\{T_H^i\}_{1 \leq i \leq N_e}$ and $\{\boldsymbol{x}_H^i\}_{1 \leq i \leq N_v}$, with N_e and N_v the number of elements and vertices, respectively. We assume that the triangulation is such that Γ^{D} and Γ^{N} consist of entire faces (edges in 2D) of $T_H \in \mathcal{T}_H$.

The corresponding finite-element approximation space is then taken to be $\boldsymbol{\mathcal{V}}_H = \{\boldsymbol{v} \in \boldsymbol{\mathcal{V}}, \boldsymbol{v}_{|T_H} \in \mathbb{P}_1(T_H), \forall T_H \in \mathcal{T}_H\}$, where $\mathbb{P}_1(T_H)$ is the space of linear polynomials over T_H. These polynomials, denoted $\{\Phi_H^i(\boldsymbol{x})\}_{1\leq i\leq N_v}$, are such that $\Phi_H^i(\boldsymbol{x}_H^j) = \delta_{ij}$, and $\text{supp}(\Phi_H^i) = \Omega_H^i$. They form a partition of unity in the sense that $\sum_{i=1}^{N_v} \Phi_H^i(\boldsymbol{x}) = 1$, $\forall \boldsymbol{x} \in \Omega$. Note that $\boldsymbol{\mathcal{V}}_H$ might be chosen to include polynomials of higher order, in relation in particular with p-finite element methods. We restrict ourselves here to this case, because it is a very popular one, and, as will be seen in Sec. 3.3, it poses specific problems.

The approximation of $\boldsymbol{u} \in \boldsymbol{\mathcal{V}}_H$ associated to $\mathcal{T}_H$, denoted $\boldsymbol{u}_H$, is then defined as the unique solution of

$$a_\Omega(\boldsymbol{u}_H, \boldsymbol{v}) = \ell(\boldsymbol{v}), \quad \forall \boldsymbol{v} \in \boldsymbol{\mathcal{V}}_H.$$

2.4 The error estimation problem

We are interested in computing the error between the exact solution $\boldsymbol{u}_{\text{ex}}$ of Eq. (3) and $\boldsymbol{u}_H$, which we will denote $\boldsymbol{z} = \boldsymbol{u}_{ex} - \boldsymbol{u}_H \in \boldsymbol{\mathcal{V}}$. By linearity, it is the solution of

$$a_\Omega(\boldsymbol{z}, \boldsymbol{v}) = \ell(\boldsymbol{v}) - a_\Omega(\boldsymbol{u}_H, \boldsymbol{v}) =: R(\boldsymbol{v}), \quad \forall \boldsymbol{v} \in \boldsymbol{\mathcal{V}}, \tag{4}$$

where the linear continuous functional $R : [\mathcal{H}^1(\Omega)]^{n_d} \to \mathbb{R}$ is called the residue, and is such that $R(\boldsymbol{v}) = 0, \forall \boldsymbol{v} \in \boldsymbol{\mathcal{V}}^H$. The resolution of Eq. (4) is of the same complexity as that of Eq. (3), because $\boldsymbol{z}$ and $\boldsymbol{v}$ are still in infinite-dimensional spaces. Therefore, we do not try to solve the problem exactly for $\boldsymbol{z}$, but rather look for bounds of $\|\boldsymbol{u}_{\text{ex}} - \boldsymbol{u}_H\|_\Omega^2 = \|\boldsymbol{z}\|_\Omega^2 = a_\Omega(\boldsymbol{z}, \boldsymbol{z}) = R(\boldsymbol{z})$.

2.5 Estimation of the error in a quantity of interest

However, in many engineering problems, the goal is rather to compute bounds on certain quantities of interest rather on the field of displacement $\|\boldsymbol{u}_{\text{ex}} - \boldsymbol{u}_H\|$. We therefore introduce that quantity of interest $s = \ell^{\mathcal{O}}$ as the output of a linear functional $\ell^{\mathcal{O}} : [\mathcal{H}^1(\Omega)]^{n_d} \to \mathbb{R}$, defined by

$$\ell^{\mathcal{O}}(\boldsymbol{v}) = \int_\Omega \boldsymbol{f}^{\mathcal{O}} \cdot \boldsymbol{v} \, d\Omega + \int_{\Gamma^{\text{N}}} \boldsymbol{g}^{\mathcal{O}} \cdot \boldsymbol{v} \, d\Gamma - a(\boldsymbol{u}^{\mathcal{O}}, \boldsymbol{v}),$$

where $\boldsymbol{f}^{\mathcal{O}} \in [\mathcal{H}^{-1}(\Omega)]^{n_d}$, $\boldsymbol{g}^{\mathcal{O}} \in [\mathcal{H}^{-\frac{1}{2}}(\Gamma^{\text{N}})]^{n_d}$, and $\boldsymbol{u}^{\mathcal{O}} \in [\mathcal{H}^{-1}(\Omega)]^{n_d}$ are three given functions. Note that this form may easily incorporate, as particular cases, displacements or tractions integrated over arbitrary subdomains or boundary segments.

Thus, our goal is to compute bounds for $\ell^{\mathcal{O}}(\boldsymbol{z})$, from which we can easily evaluate the bounds for $s_{\text{ex}} = \ell^{\mathcal{O}}(\boldsymbol{u}_{\text{ex}}) = s_H + \ell^{\mathcal{O}}(\boldsymbol{z})$ as

$$s_H + s_H^{\text{low}} \leq s_{\text{ex}} \leq s_H + s_H^{\text{up}},$$

where $s_H = \ell^{\mathcal{O}}(\boldsymbol{u}_H)$, and s_H^{up} and s_H^{low} are, respectively, upper and lower bounds for $\ell^{\mathcal{O}}(\boldsymbol{z})$.

Different methods [2, 18] exist to compute s_H^{up} and s_H^{low}, usually based on the computation of the bounds of the energy norm of the solution of a dual problem with the same structure as Eq. (4). We will therefore concentrate in this paper on the bounding of the energy norm of $\boldsymbol{z}$, solution of Eq. (4), and assume that it allows us to bound s_{ex}. The applications in Section 5 will however present bounds on quantities of interest.

Finally, it is customary to introduce the estimated value s_H^{est} of s_{ex} as the mean value between the two bounds

$$s_H^{\text{est}} = s_H + \frac{s_H^{\text{up}} + s_H^{\text{low}}}{2},$$

and the relative bound gap as

$$\rho_H = 2\frac{s_H^{\text{up}} - s_H^{\text{low}}}{s_H^{\text{est}}}.$$

When no exact solution is available, that is to say for all interesting situations, ρ_H can be used to judge the accuracy of the bounds.

3 Asymptotic error estimation

As described above, Eq. (4) cannot be solved exactly because it is posed in an infinite-dimensional space. The idea behind asymptotic error estimation methods is to replace the exact problem (4) by a discretized version using a triangulation, $\mathcal{T}_h$, much finer than $\mathcal{T}_H$, and a corresponding finite element approximation space of functions $\boldsymbol{\mathcal{V}}_h = \{\boldsymbol{v} \in \boldsymbol{\mathcal{V}}, \boldsymbol{v}_{|T_h} \in \mathbb{P}_1(T_h), \forall T_h \in \mathcal{T}_h\}$. The refined approximation to $\boldsymbol{z}_h$ of $\boldsymbol{z}$, is given by

$$a(\boldsymbol{z}_h, \boldsymbol{v}) = \ell(\boldsymbol{v}), \quad \forall \boldsymbol{v} \in \boldsymbol{\mathcal{V}}_h.$$

Even when $h \ll H$, and $\boldsymbol{z}_h$ can be considered a good approximation of $\boldsymbol{z}$, it should be stressed that all bounds that are derived in this section really make reference to $\|\boldsymbol{z}_h\|_\Omega$ and not $\|\boldsymbol{z}\|_\Omega$.

The next two sections introduce the basis of the subdomain-based flux-free approach, as described in particular in [15, 10]. The problem of the solvability of the local problems, already discussed in these references, is then completed by the description of a new projection operator.

3.1 Definition of the subdomains

The subdomains where the local problems will be defined are the stars (or patches)

$$\Omega_H^i = \bigcup_{j=1}^{N_e} \delta\left(\boldsymbol{x}_H^i \in \overline{T_H^j}\right) T_H^j, \quad 1 \leq i \leq N_v,$$

that are the unions of elements in contact with one vertex. This definition leads us to the introduction of a new functional space for each star,

$$\boldsymbol{\mathcal{V}}_{\Omega_H^i}^H = \boldsymbol{\mathcal{V}}^H \cap [\mathcal{H}^1(\Omega_H^i)]^{n_d},$$

which formally contains continuous functions defined over Ω_H^i, and that we extend to Ω by setting the undefined values to zero. The functions in each of these spaces are therefore continous over Ω_H^i but discontinous over Ω. We introduce, in a similar manner, $\boldsymbol{\mathcal{V}}_{\text{brok}} = \oplus_{i=1}^{N_e} (\boldsymbol{\mathcal{V}} \cap [\mathcal{H}^1(T_H^i)]^{n_d})$, which contains functions that are continuous in each element of the triangulation $\mathcal{T}_H$, but generally discontinous across the inter-element faces. We additionally notice that $\boldsymbol{\mathcal{V}}_{\Omega_H^i}^H \subset \boldsymbol{\mathcal{V}}_{\text{brok}}$, $1 \leq i \leq N_v$.

3.2 Definition of the local problems

The subdomain-based flux-free error estimation method relies on the properties of the Finite Element interpolation functions $\{\Phi_H^i(\boldsymbol{x})\}_{1 \leq i \leq N_v}$, which form a partition of unity over Ω. One can therefore write Eq. (4) as

$$a(\boldsymbol{z}, \boldsymbol{v}) = R(\boldsymbol{v}) = R\left(\sum_{i=1}^{N_v} \Phi_H^i \boldsymbol{v}\right) = \sum_{i=1}^{N_v} R(\Phi_H^i \boldsymbol{v}), \quad \forall \boldsymbol{v} \in \boldsymbol{\mathcal{V}}.$$

We consider the local error estimation problems consisting in finding, for $1 \leq i \leq N_v$, the local $\boldsymbol{z}^i \in \boldsymbol{\mathcal{V}}_{\Omega_H^i}^H$ solution of

$$a_i(\boldsymbol{z}^i, \boldsymbol{v}) = R(\Phi_H^i \boldsymbol{v}), \quad \forall \boldsymbol{v} \in \boldsymbol{\mathcal{V}}_{\Omega_H^i}^H, \quad 1 \leq i \leq N_v, \tag{5}$$

where the linear continuous functionals $a_i : [\mathcal{H}^1(\Omega_H^i)]^{n_d} \times [\mathcal{H}^1(\Omega_H^i)]^{n_d} \to \mathbb{R}$ are the restrictions on Ω_H^i of a, such that

$$a_i(\boldsymbol{w}, \boldsymbol{v}) = \int_{\Omega_H^i} \boldsymbol{\sigma}(\boldsymbol{w}) : \boldsymbol{\epsilon}(\boldsymbol{v}) \, d\Omega, \quad 1 \leq i \leq N_v.$$

It can be seen that the support of $\Phi_H^i \boldsymbol{v}$ is the star Ω_H^i so that each Eq. (5) is indeed local. Once these N_v local problems have been solved, the error estimator $\hat{\boldsymbol{z}}$ defined by

$$\hat{\boldsymbol{z}} = \sum_{i=1}^{N_v} \boldsymbol{z}^i \tag{6}$$

can be proved to verify $\|\boldsymbol{z}\|_\Omega \leq \|\hat{\boldsymbol{z}}\|_\Omega$. It should be noted that $\hat{\boldsymbol{z}} \in \boldsymbol{\mathcal{V}}_{\text{brok}}$, so that it is only continuous by parts, on each of the elements, and not continuous over Ω.

3.3 Solvability of the local problems

In order for the local problems (5) to be solvable, we must verify that

$$R(\Phi_H^i \boldsymbol{v}) = 0, \quad \forall \boldsymbol{v} \in \ker a_i. \tag{7}$$

Physically, $\ker a_i$ groups the rigid body displacement fields over the star Ω_H^i. They are at most linear over the star. When considering high-order polynomials for the resolution of

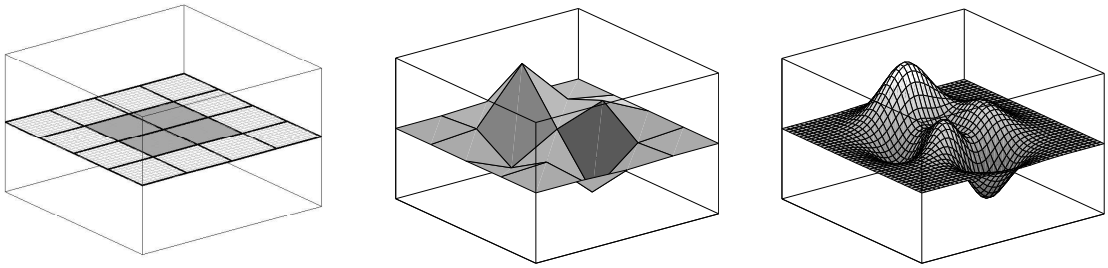

Figure 2: Two conforming finite element meshes with different refinement (left) with one star indicated (left, darker shade); and test function interpolated on the coarse (center) and refined (right) meshes.

the original problem, that is when $\boldsymbol{\mathcal{V}}^H$ contains the second-order polynomials (by parts), $R(\Phi_H^i \boldsymbol{v})$ is then null, when $\boldsymbol{v}$ is one of these rigid body fields. However, when using first order polynomials at most over the elements, $\Phi_H^i \boldsymbol{v}$ is not necessarily included in $\boldsymbol{\mathcal{V}}^H$, so that Eq. (7) is not necessarily verified.

In order to ensure the solvability of the local problems, the introduction of a projection operator $\Pi : \boldsymbol{\mathcal{V}} \to \boldsymbol{\mathcal{V}}^H$ was proposed in [10], such that

$$R\left(\Pi \boldsymbol{v}\right) = \sum_{i=1}^{N_v} R\left(\Phi_i \Pi \boldsymbol{v}\right) = 0, \quad \forall \boldsymbol{v} \in \boldsymbol{\mathcal{V}}.$$

It should be remembered that such a projection operator verifies, by definition, $\Pi \boldsymbol{v} = \boldsymbol{v}$, $\forall \boldsymbol{v} \in \boldsymbol{\mathcal{V}}^H$. If we rewrite then Eq. (5) as

$$a_i(\boldsymbol{z}^i, \boldsymbol{v}) = R\left(\Phi_H^i(\boldsymbol{v} - \Pi \boldsymbol{v})\right), \quad \forall \boldsymbol{v} \in \boldsymbol{\mathcal{V}}^H_{\Omega_H^i}, \quad 1 \leq i \leq N_v, \tag{8}$$

we see that $\hat{\boldsymbol{z}}$, defined in Eq. (6), still provides the desired bound, while ensuring the solvability of each local problem, even when considering linear interpolating polynomials for $\boldsymbol{\mathcal{V}}^H$. The next two sections present two such projection operators. For each of them, we will also derive the adjoint operators $\Pi^{\Omega *}$ and $\Pi^{\Gamma^N *}$, in the sense defined in Sec. 2.

To observe and compare the properties of these two projection operators, a simple example is provided. In Fig. 2, a pair of simple coarse and refined meshes in $\mathbb{R}^2$ is presented, along with the interpolation of a test function on each of the meshes. This function can be imagined, for example, to be one component of a displacement field or volume force field. Fig. 3 and Fig. 4 then depict, respectively, the action of the projection operators on a displacement field, and that of their adjoint on a volume force field.

3.3.1 Pointwise projection operator

The pointwise projection operator $\Pi_0 : \boldsymbol{\mathcal{V}} \to \boldsymbol{\mathcal{V}}^H$ is defined by

$$\Pi_0 \boldsymbol{v}(\boldsymbol{x}) = \sum_{i=1}^{N_v} \Phi_H^i(\boldsymbol{x}) \boldsymbol{v}(\boldsymbol{x}_H^i).$$

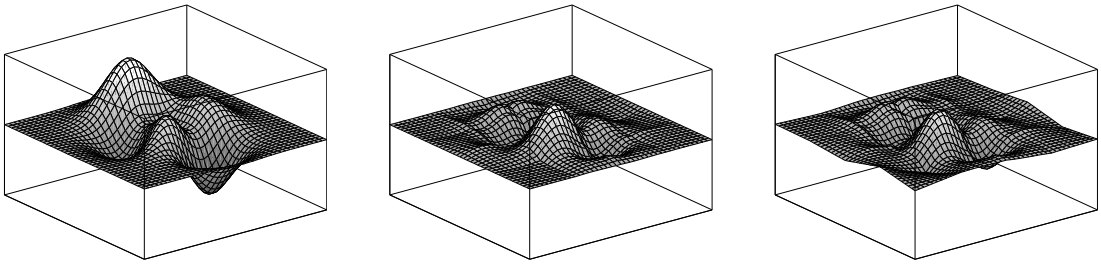

Figure 3: Test function $\boldsymbol{v}$ (left) and quantity $(\mathrm{Id}-\Pi)\boldsymbol{v}$ for the pointwise projection operator Π_0 (center) and the global linear operator Π (right).

It can be easily seen that $\Pi_0\boldsymbol{v}(\boldsymbol{x}_H^i) = \boldsymbol{v}(\boldsymbol{x}_H^i)$, $\forall 1 \leq i \leq N_v$, so that $\Pi_0\boldsymbol{v}$ is the linear interpolant of $\boldsymbol{v}$ at the vertices of the finite element mesh. The adjoint operators $\Pi_0^{\Omega *}$ and $\Pi_0^{\Gamma^{\mathrm{N}} *}$ are defined by

$$\Pi_0^{\Omega *}\boldsymbol{f} = \sum_{i=1}^{N_v} \delta(\boldsymbol{x}-\boldsymbol{x}_i) \int_\Omega \Phi_H^i \boldsymbol{f}\, d\Omega,$$

and

$$\Pi_0^{\Gamma^{\mathrm{N}} *}\boldsymbol{g} = \sum_{i=1}^{N_v} \delta(\boldsymbol{x}-\boldsymbol{x}_i) \int_{\Gamma^{\mathrm{N}}} \Phi_H^i \boldsymbol{g}\, d\Omega.$$

Indeed, with these definitions, it can be checked that $\langle \boldsymbol{f}, \Pi_0\boldsymbol{v}\rangle_\Omega = \langle \Pi_0^{\Omega *}\boldsymbol{f}, \boldsymbol{v}\rangle_\Omega$, and $\langle \boldsymbol{g}, \Pi_0\boldsymbol{v}\rangle_{\Gamma^{\mathrm{N}}} = \langle \Pi_0^{\Gamma^{\mathrm{N}} *}\boldsymbol{g}, \boldsymbol{v}\rangle_\Omega$. When considering the strong formulation in section 4.1, these definitions for the adjoint operators will lead to the introduction of concentrated forces, which are complex to deal with in a numerical setting. We therefore introduce another projection operator, with smoother adjoint.

3.3.2 Global linear projection operator

The global linear projection operator $\Pi_\Omega : \boldsymbol{\mathcal{V}} \to \boldsymbol{\mathcal{V}}^H$ is defined by

$$\Pi_\Omega\boldsymbol{v}(\boldsymbol{x}) = \sum_{i=1}^{N_v} \Psi_H^i(\boldsymbol{x}) \int_\Omega \Phi_H^i \boldsymbol{v}\, d\Omega = \sum_{i=1}^{N_v} \Phi_H^i(\boldsymbol{x}) \int_\Omega \Psi_H^i \boldsymbol{v}\, d\Omega,$$

where the $\{\Psi_H^i\}_{1\leq i\leq N_v}$ are defined by

$$\Psi_H^i = \sum_{j=1}^{N_v} [M^{-1}]_{ij}\, \Phi_H^j(\boldsymbol{x}), \quad 1 \leq i \leq N_v,$$

with $[M^{-1}]$ the inverse of the mass matrix $[M]$ defined by

$$[M]_{ij} = \int_\Omega \Phi_H^i \Phi_H^j\, d\Omega, \quad 1 \leq i,j \leq N_v.$$

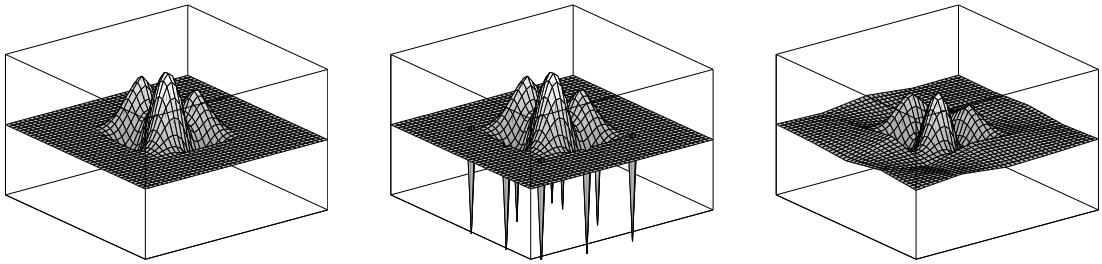

Figure 4: Dual test function weighted on the star $\Phi_H^i \boldsymbol{f}$ (left), and quantity $(\mathrm{Id}-\Pi\ ^*)(\Phi_H^i \boldsymbol{f})$ corresponding to the pointwise projection operator Π_0 (center) and the global linear operator $\Pi\quad$ (right).

The functions $\{\Psi_H^i\}_{1\leq i\leq N_v}$ are linear over each element T_H, like the $\{\Phi_H^i\}_{1\leq i\leq N_v}$, however their support is not limited to one star, but extends in general over the entire domain Ω. This is related to the fact that, although $[M]$ is local, in the sense that it is mainly filled with null entries, its inverse $[M^{-1}]$ is not. It should be noted that the introduction of this global operator might be thought to go against the general philosophy of localization in subdomain-based computations. However, we will see in Section 4 that this is not the case as the operator Π_Ω will always go accompanied by a localizing function.

An interesting property of this operator is that it minimizes the L^2-norm in the sense that, for any $\boldsymbol{w} : \boldsymbol{\mathcal{V}} \to \boldsymbol{\mathcal{V}}^H$, $\|\Pi \boldsymbol{v} - \boldsymbol{v}\|_{L^2}^2 \leq \|\boldsymbol{w} - \boldsymbol{v}\|_{L^2}^2$.

Finally, we observe that Π_Ω is self-adjoint in the sense that, for all $\boldsymbol{f} \in [\mathcal{H}^{-1}(\Omega)]^{n_d}$ and $\boldsymbol{v} \in [\mathcal{H}^1(\Omega)]^{n_d}$,

$$\langle \boldsymbol{f}, \Pi_\Omega \boldsymbol{v} \rangle_\Omega = \langle \Pi_\Omega \boldsymbol{f}, \boldsymbol{v} \rangle_\Omega = \langle \Pi_\Omega^{\Omega *} \boldsymbol{f}, \boldsymbol{v} \rangle_\Omega,$$

and we have that

$$\Pi_\Omega^{\Gamma^{\mathrm{N}} *} \boldsymbol{g}(\boldsymbol{x}) = \sum_{i=1}^{N_v} \Psi_H^i(\boldsymbol{x}) \int_{\Gamma^{\mathrm{N}}} \Phi_H^i \boldsymbol{v}\ d\Omega = \sum_{i=1}^{N_v} \Phi_H^i(\boldsymbol{x}) \int_{\Gamma^{\mathrm{N}}} \Psi_H^i \boldsymbol{v}\ d\Omega,$$

as it is easy to check that, for all $\boldsymbol{g} \in [\mathcal{H}^{-1/2}(\Omega)]^{n_d}$ and $\boldsymbol{v} \in [\mathcal{H}^1(\Omega)]^{n_d}$, $\langle \Pi_\Omega^{\Gamma^{\mathrm{N}} *} \boldsymbol{g}, \boldsymbol{v} \rangle_\Omega = \langle \boldsymbol{g}, \Pi_\Omega \boldsymbol{v} \rangle_{\Gamma^{\mathrm{N}}}$.

4 Strict error estimation

A dual formulation based on the principle of minimizing the complementary energy is used to obtain computable approximations of the solutions of a series of local problems that, once combined, provide an upper bound of the exact error. This method extends previous works in the context of hybrid-flux residual estimators [16, 17] to the flux-free methodology.

4.1 Strong form of the residual global problem

We first explicitate the weak formulation of the global problem, and derive the corresponding strong formulation. Expanding Eq. (4), it is recalled that the weak formulation of the residual global problem states: find $\boldsymbol{u} \in \boldsymbol{\mathcal{V}}$ such that

$$\int_\Omega \boldsymbol{\sigma}(\boldsymbol{z}) : \boldsymbol{\epsilon}(\boldsymbol{v})\, d\Omega = \int_\Omega \boldsymbol{f} \cdot \boldsymbol{v}\, d\Omega + \int_{\Gamma^{\mathrm{N}}} \boldsymbol{g} \cdot \boldsymbol{v}\, d\Gamma - \int_\Omega \boldsymbol{\sigma}(\overline{\boldsymbol{u}_H}) : \boldsymbol{\epsilon}(\boldsymbol{v})\, d\Omega, \quad \forall \boldsymbol{v} \in \boldsymbol{\mathcal{V}},$$

where $\overline{\boldsymbol{u}_H} = \boldsymbol{u}_H + \boldsymbol{u}^{\mathrm{D}}$. Integrating by parts, and taking into account the discontinuity of the stress field at the interfaces between the elements, we get the strong form of the residual global problem:

$$\begin{cases} \mathrm{Div}_{\boldsymbol{x}} \boldsymbol{\sigma}(\boldsymbol{z}) + (\boldsymbol{f} + \mathrm{Div}_{\boldsymbol{x}} \boldsymbol{\sigma}(\overline{\boldsymbol{u}_H})) = \boldsymbol{0} & \text{in } \Omega \\ \boldsymbol{\sigma}(\boldsymbol{z}) \cdot \boldsymbol{n} - (\boldsymbol{g} - \boldsymbol{\sigma}(\overline{\boldsymbol{u}_H}) \cdot \boldsymbol{n}) = \boldsymbol{0} & \text{on } \Gamma^{\mathrm{N}} \\ [\![\boldsymbol{\sigma}(\boldsymbol{z}) \cdot \boldsymbol{n}]\!] + [\![\boldsymbol{\sigma}(\overline{\boldsymbol{u}_H}) \cdot \boldsymbol{n}]\!] = \boldsymbol{0} & \text{on } \Gamma_{\mathrm{int}} \\ \boldsymbol{z} = \boldsymbol{0} & \text{on } \Gamma^{\mathrm{D}} \end{cases}.$$

4.2 Dual formulation of the global problem

The dual formulation consists in introducing a new variable $\boldsymbol{q}$, in the space of second-order tensors with coordinates in $L^2(\Omega)$, representing a stress field that verifies

$$\begin{cases} \mathrm{Div}_{\boldsymbol{x}} \boldsymbol{q} = -\boldsymbol{f}_H & \text{in } \Omega \\ \boldsymbol{q} \cdot \boldsymbol{n} = \boldsymbol{g}_H & \text{on } \Gamma^{\mathrm{N}} \\ [\![\boldsymbol{q} \cdot \boldsymbol{n}]\!] = -\boldsymbol{j}_H & \text{on } \Gamma_{\mathrm{int}} \end{cases},$$

and is said to be statically admissible. We posed $\boldsymbol{f}_H = \boldsymbol{f} + \mathrm{Div}_{\boldsymbol{x}} \boldsymbol{\sigma}(\overline{\boldsymbol{u}_H})$, $\boldsymbol{g}_H = \boldsymbol{g} - \boldsymbol{\sigma}(\overline{\boldsymbol{u}_H})$, $\boldsymbol{j}_H = [\![\boldsymbol{\sigma}(\overline{\boldsymbol{u}_H}) \cdot \boldsymbol{n}]\!]$ and we additionally define the complementary energy as

$$\pi_c(\boldsymbol{q}) = \frac{1}{2} \int_\Omega \boldsymbol{q} : \mathbb{C}^{-1} : \boldsymbol{q}\, d\Omega.$$

It can be verified, using Cauchy-Schwartz's inequality, that any such field provides an upper bound for the energy norm of the error as

$$2\pi_c(\boldsymbol{q}) \geq \|\boldsymbol{z}\|_\Omega^2.$$

and that the equality is obtained for $\boldsymbol{q} = \boldsymbol{\sigma}(\boldsymbol{z})$.

In [17, Appendix A], a constructive proof is given of the existence of such a statically admissible stress field on each element of the finite element mesh, provided that the loads (volume and surface) be polynomial by parts. We extend this now to the context of the flux-free methodology.

4.3 Strong form of the local problems

We propose to apply the same methodology as above, but this time on each of the local problems (8) defined over the stars. We therefore turn to the expansion of the weak form in Eq. (8), which reads: find $\boldsymbol{z}^i \in \boldsymbol{\mathcal{V}}^H_{\Omega^i_H}$ such that

$$\int_{\Omega^i_H} \boldsymbol{\sigma}(\boldsymbol{z}^i) : \boldsymbol{\epsilon}(\boldsymbol{v})\, d\Omega = \int_{\Omega^i_H} \boldsymbol{f} \cdot \Phi^i_H(\mathrm{Id}-\Pi)\boldsymbol{v}\, d\Omega + \int_{\Gamma^{\mathrm{N}}\cap\partial\Omega^i_H} \boldsymbol{g} \cdot \Phi^i_H(\mathrm{Id}-\Pi)\boldsymbol{v}\, d\Gamma - \int_{\Omega^i_H} \boldsymbol{\sigma}(\overline{\boldsymbol{u}_H}) : \boldsymbol{\epsilon}(\Phi^i_H(\mathrm{Id}-\Pi)\boldsymbol{v})\, d\Omega,\ \forall \boldsymbol{v} \in \boldsymbol{\mathcal{V}}^H_{\Omega^i_H},$$

where Π may represent either Π_0 or Π_Ω.

The corresponding strong form, using the adjoints $\Pi^{\Omega *}$, $\Pi^{\Gamma^{\mathrm{N}} *}$, and $\Pi^{\Gamma_{\mathrm{int}} *}$ (defined similarly to $\Pi^{\Gamma^{\mathrm{N}} *}$, only replacing the boundary) of Π, and the previously defined loads $\boldsymbol{f}_H$, $\boldsymbol{g}_H$ and $\boldsymbol{j}_H$, is

$$\begin{cases} \mathrm{Div}_{\boldsymbol{x}}\boldsymbol{\sigma}(\boldsymbol{z}^i) = (\Pi^{\Omega *} - \mathrm{Id})(\Phi^i_H \boldsymbol{f}_H) - \Pi^{\Gamma^{\mathrm{N}} *}(\Phi^i_H \boldsymbol{g}_H) + \Pi^{\Gamma_{\mathrm{int}} *}(\Phi^i_H \boldsymbol{j}_H) & \text{in } \Omega^i_H \\ \boldsymbol{\sigma}(\boldsymbol{z}^i)\cdot\boldsymbol{n} = \Phi^i_H \boldsymbol{g}_H & \text{on } \Gamma^{\mathrm{N}} \cap \partial\Omega^i_H \\ [\![\boldsymbol{\sigma}(\boldsymbol{z}^i)\cdot\boldsymbol{n}]\!] = -\Phi^i_H \boldsymbol{j}_H & \text{on } \Gamma_{\mathrm{int}} \\ \boldsymbol{z}^i = \boldsymbol{0} & \text{on } \Gamma^{\mathrm{D}} \cap \partial\Omega^i_H \end{cases}.$$

4.4 Dual formulation of the local problems

For the dual formulation of the local problems, we therefore seek, on each star, a statically admissible field $\boldsymbol{q}^i$ verifying

$$\begin{cases} \mathrm{Div}_{\boldsymbol{x}}\boldsymbol{q}^i = (\Pi^{\Omega *} - \mathrm{Id})(\Phi^i_H \boldsymbol{f}_H) - \Pi^{\Gamma^{\mathrm{N}} *}(\Phi^i_H \boldsymbol{g}_H) + \Pi^{\Gamma_{\mathrm{int}} *}(\Phi^i_H \boldsymbol{j}_H) & \text{in } \Omega^i_H \\ \boldsymbol{q}^i\cdot\boldsymbol{n} = \Phi^i_H \boldsymbol{g}_H & \text{on } \Gamma^{\mathrm{N}} \cap \partial\Omega^i_H \\ [\![\boldsymbol{q}^i\cdot\boldsymbol{n}]\!] = -\Phi^i_H \boldsymbol{j}_H & \text{on } \Gamma_{\mathrm{int}} \end{cases}.$$

If we particularize the projection operator for the two cases that were studied in the previous sections, we see that Π_0 leads to the introduction of punctual forces in the definition of the local problems above, while Π_Ω leads to the introduction of linear loads distributed in the volume Ω^i_H. The results that are described in [17] can therefore be readily extended to the flux-free formulation when using the projection operator Π_Ω. In that case, a statically admissible $\boldsymbol{q}^i$ can be computed on each star, which results in global statically admissible stress field by summation. We then have the strict upper bound for the energy norm of the error:

$$2\pi_c(\hat{\boldsymbol{q}}) = 2\pi_c\left(\sum_{i=1}^{N_v} \boldsymbol{q}^i\right) \geq \|\boldsymbol{z}\|^2_\Omega. \tag{9}$$

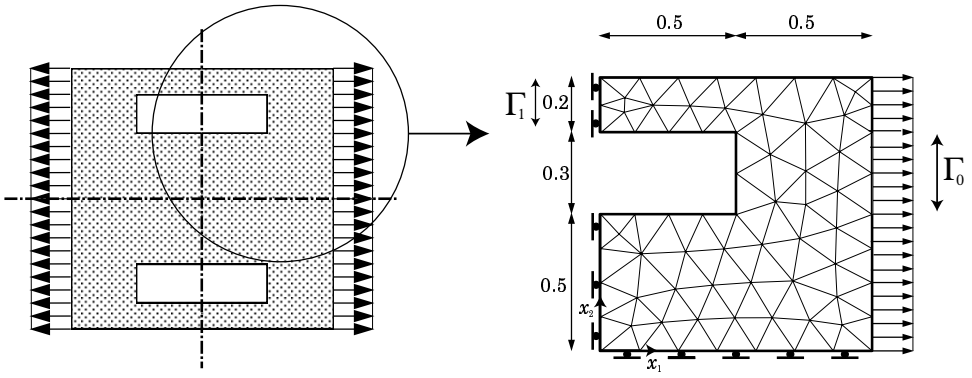

Figure 5: Geometry of the 2D square plate with rectangular holes (left), and initial mesh of the one-fourth part that is considered for modelling (right). Γ_0 defines the part of the boundary on which the displacement is integrated to yield the output quantity of interest. These drawings were extracted from [19].

5 Application: 2D Square plate with rectangular holes

A square thin plate with rectangular holes is considered. Normal tractions are applied on the left and right sides of the plate. Since the problem is symmetric, only one fourth of the plate is considered, as shown in Fig. 5. This problem was already studied in [19, 20, 15, 17] using `tri3` elements and in [10] using `quad4` elements, each time coupled with adaptivity schemes. Here we consider a series of uniformly refined meshes by starting at an value of the mesh diameter $h_{ini} \approx 0.14$, and successively adding a node at the center of each segment, replacing each triangle by four smaller ones.

The output of interest that is considered is the integral of the normal displacement over the boundary Γ_0, that is

$$\ell^{\mathcal{O}}(\boldsymbol{v}) = \int_{\Gamma_0} \boldsymbol{v} \cdot \boldsymbol{n} \, d\Gamma.$$

Fig. 6 and Tab. 1 show the convergence of the bounds and of the relative bound gap for this problem.

6 Conclusions and perspectives

In this paper, we have described the extension of previous results on the derivation of strict bounds for the energy norm of the error to the framework of the flux-free method. The main novelty lies in the introduction of a new projection operator that, at the same time, ensures the solvability of the local problems posed on the stars, and allows for the construction of the statically admissible fields required for the estimation of the strict bounds.

Further, this global projection operator will also allow for the construction of strict bounds in nonlinear problems, when some classical conditions of convexity or monotonicity

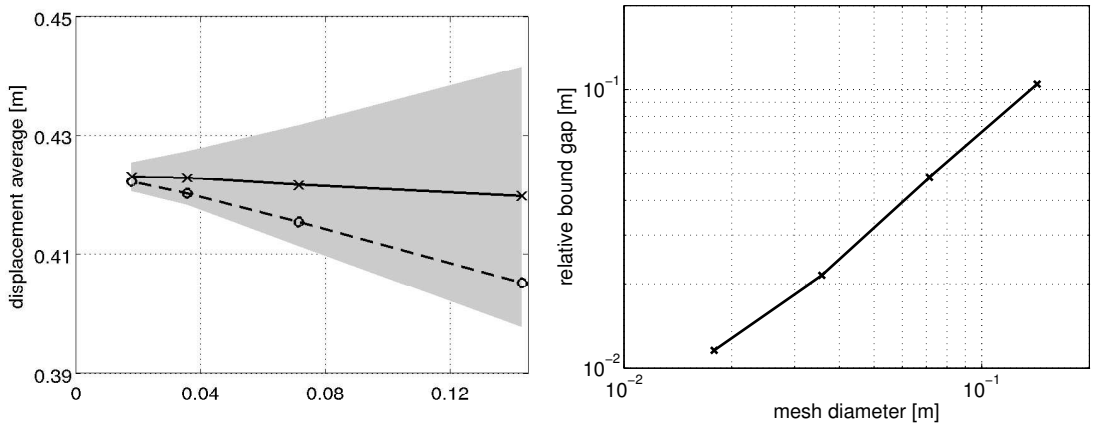

Figure 6: Finite-Element approximation s_H (left, dashed line), estimated value s_H^{est} (left, solid line) and bounds (left, gray shade); and relative bound gap (right) in a series of uniformly refined h-meshes for $\ell^{\mathcal{O}}(\boldsymbol{u}_H)$

mesh diameter [m]	Nb. elts. [-]	displacement [m]				
h	N_e	s_H	s_H^{est}	s_H^{low}	s_H^{up}	ρ_H
$\text{h}_{\text{ini}} \approx 0.14$	108	.4051	.4197	-.0074	.0365	.1046
$\text{h}_{\text{ini}}/2$	1728	.4153	.4215	-.0040	.0164	.0484
$\text{h}_{\text{ini}}/4$	6912	.4201	.4227	-.0019	.0072	.0215
$\text{h}_{\text{ini}}/8$	27648	.4221	.4229	-.0016	.0033	.0116

Table 1: Bounds and relative bound gap in a series of uniformly refined h-meshes for $\ell^{\mathcal{O}}(\boldsymbol{u}_H)$

are verified, and following the works in [21, 22, 23]. Indeed, in these references, the derivation of strict bounds is mainly based on the construction of a statically admissible stress field, which has now been made possible within the framework of the flux-free methodology.

Con el apoyo de *Universitat Politècnica de Catalunya* y *E.T.S. d'Enginyers de Camins, Canals i Ports de Barcelona*

REFERENCES

[1] I. Babu**v**ska and J. T. Oden. Verification and validation in computational engineering and science: basic concepts. *Comp. Meths. Appl. Mech. Engr.*, 193:4057–4066, 2004.

[2] M. Ainsworth and J. T. Oden. *A posteriori error estimation in finite element analysis.* Pure and Applied Mathematics. Wiley-Interscience, 2000.

[3] P. Ladevèze and J.-P. Pelle. *Mastering calculations in linear and nonlinear mechanics.* Mechanical Engineering. Springer, 2005.

[4] O. C. Zienkiewicz and J. Z. Zhu. A simple error estimator and adaptive procedure for practical engineering analysis. *Int. J. Numer. Meth. Engr.*, 24:337–357, 1987.

[5] I. Babu**v**ska and W. C. Rheinboldt. Error estimates for adaptive finite element computations. *SIAM J. Numer Anal.*, 15(4):736–755, 1978.

[6] I. Babu**v**ska and W. C. Rheinboldt. A posteriori error estimates for the finite element method. *Int. J. Numer. Meth. Engr.*, 12(10):1597–1615, 1978.

[7] P. Ladevèze and D. Leguillon. Error estimate procedure in the finite element method and applications. *SIAM J. Numer Anal.*, 20(3):485–509, 1983.

[8] L. Demkowicz, J. T. Oden, and T. Strouboulis. Adaptative finite elements for flow problems with moving boundaries. Part I: variational principles and a posteriori error estimates. *Comp. Meths. Appl. Mech. Engr.*, 46(2):217–251, 1984.

[9] H.-W. Choi and M. Paraschivoiu. Adaptive computations of a posteriori finite element output bounds: a comparison of the 'hybrid-flux' approach and the 'flux-free' approach. *Comp. Meths. Appl. Mech. Engr.*, 193(36-38):4001–4033, 2004.

[10] N. Parés, P. Díez, and A. Huerta. Subdomain-based flux-free a posteriori error estimators. *Comp. Meths. Appl. Mech. Engr.*, 195(4-6):297–323, 2006.

[11] C. Carstensen and S. A. Funken. Fully reliable localized error control in the FEM. *SIAM Journal on Scientific Computing*, 21(4):1465–1484, 1999-2000.

[12] L. Machiels, Y. Maday, and A. T. Patera. A 'flux-free' nodal Neumann subproblem approach to output bounds for partial differential equations. *Comptes-Rendus de l'Académie des Sciences - Series I - Mathematics*, 330(3):249–254, 2000.

[13] P. Morin, R. H. Nochetto, and K. G. Siebert. Local problems on stars: a posteriori error estimators, convergence, and performance. *Mathematics of Computation*, 72:1067–1097, 2003.

[14] S. Prudhomme, F. Nobile, L. Chamoin, and J. T. Oden. Analysis of a subdomain-based error estimator for finite element approximations of elliptic problems. *Numer. Meths. Part. Diff. Eqs.*, 20(2):165–192, 2004.

[15] N. Parés. *Error assessment for functional outputs of PDE's: bounds and goal-oriented adaptivity.* PhD thesis, Universitat Politécnica de Catalunya, Barcelona, Spain, 2005.

[16] A. M. Sauer-Budge, J. Bonet, A. Huerta, and J. Peraire. Computing bounds for linear functionals of exact weak solutions to Poisson's equation. *SIAM J. Numer Anal.*, 42(4):1610–1630, 2004.

[17] N. Parés, J. Bonet, A. Huerta, and J. Peraire. The computation of bounds for linear-functional outputs of weak solutions to the two-dimensional elasticity equations. *Comp. Meths. Appl. Mech. Engr.*, 195(4-6):406–429, 2006.

[18] P. Díez, N. Parès, and A. Huerta. Recovering lower bounds of the error postprocessing implicit residual a posteriori error estimates. *Int. J. Numer. Meth. Engr.*, 56(10):1465–1488, 2003.

[19] J. Peraire and A. T. Patera. Bounds for linear-functional outputs of coercive partial differential equations: local indicators and adaptive refinement. In Pierre Ladevèze and J. Tinsley Oden, editors, *Workshop On New Advances in Adaptive Computational Methods in Mechanics*, 1997.

[20] M. Paraschivoiu, J. Peraire, and A. T. Patera. A posteriori finite element bounds for linear-functional outputs of elliptic partial differential equations. *Comp. Meths. Appl. Mech. Engr.*, 150(1-4):23–50, 1997.

[21] P. Ladevèze. Upper error bound on calculated outputs of interest for linear and nonlinear structural problems. *Comptes Rendus Mécanique*, 334:399–407, 2006.

[22] P. Ladevèze. Strict upper error bounds on computed outputs of interest in computational structural mechanics. *Comp. Mech.*, Available online, 2007.

[23] L. Chamoin and P. Ladevèze. Bounds on history-dependent or independent local quantities in viscoelasticity problems solved by approximate methods. *Int. J. Numer. Meth. Engr.*, 71:1387–1411, 2007.